Binuclear Copper Complexes Based on the 6,6′-Bis[[bis(2-pyridylmethyl)amino]methyl]-2,2′-bipyridine Ligand

Dong-Heon Lee, Narasimha N. Murthy, and Kenneth D. Karlin*

Department of Chemistry, The Johns Hopkins University, Charles and 34th Streets, Baltimore, Maryland 21218

Received May 29, 1997[⊗]

The tripodal tetradentate ligand TMPA (tris(2-pyridylmethyl)amine) has provided a wealth of valuable new Cu(I) and Cu(II) chemistry, in particular associated with copper(I)/dioxygen reactivity studies (Karlin, K. D.; Kaderli, S.; Zuberbühler, A. D. *Acc. Chem. Res.* **1997**, *30*, 139−147). Dinucleating analogues have also been recently investigated, and here we describe new copper complexes of the 6,6′-bis[[bis(2-pyridylmethyl)amino]methyl]-2,2′-bipyridine ligand (bTMPA). The synthesis and X-ray crystallographic characterization of $[(bTMPA)Cu^{II}_2(CH_3CN)_2(ClO_4)_2]^{2+}$ (**1**, as ClO_4^- salt) and $[(bTMPA)Cu^{II}_2(N_3)_2(ClO_4)_2]$ (**2**) are provided. [**1:** space group $C2/c$; a = 15.907(4) Å, b = 29.268(7) Å, c = 13.941(2) Å; β = 97.79(2)°; Z = 4; volume = 6431(2) Å^3. **2**: space group $P2_1/c$; a = 8.118(5) Å, b = 29.743(8) Å, c = 9.120(6) Å; β = 114.00(5)°; Z = 2; volume = 2012(2) Å^3.] Both solid state structures possess six-coordinate copper(II) ions, and in neither case does the 2,2′-bipyridine (bipy) moiety within bTMPA chelate to a single metal ion. Dissociation of bound perchlorate and the presence of pentacoordinate solution structures are suggested by spectroscopic (UV−vis with two d−d absorptions; axial EPR spectra) along with conductivity data (**1**, 1:4 electrolyte; **2**, 1:2 electrolyte). Electrochemical measurements by cyclic volammetry have been carried out, and for a dicopper(I) analogue, $[(bTMPA)Cu^{I}_2](ClO_4)_2$ (**3**$(ClO_4)_2$), a single quasireversible redox wave is observed; $E_{1/2}$ = +199 mV (versus Ag/AgCl in dimethylformamide), which is ∼280 mV more positive than that observed for the simple "parent" compound $[Cu^{I}(TMPA)(CH_3CN)](ClO_4)$. Unlike $[Cu^{I}(TMPA)(CH_3CN)](ClO_4)$, **3** does not readily form dioxygen adducts.

Introduction

There has been considerable interest in the synthesis, structures, redox properties, and dioxygen reactivity of dicopper(I) and related dicopper(II) compounds, as potential models for dicopper centers observed in the active sites of metalloenzymes such as hemocyanin (O_2 carrier) and tyrosinase (*o*-phenol monooxygenase).[1,2] In particular, copper complexes of TMPA (tris(2-pyridylmethyl)amine) (Chart 1) and related ligands have been particularly useful in studying fundamental aspects of copper(I)/dioxygen reactivity. The mononuclear copper(I) complex $[(TMPA)Cu^{I}(RCN)]^+$ (R = Me, Et) reacts reversibly with O_2 to form a low-temperature (i.e., −80 °C) stable complex $[\{(TMPA)Cu\}_2(O_2)]^{2+}$, possessing a *trans*-($\mu$-1,2-peroxo)dicopper(II) physical and electronic structure.[3,4] Detailed thermodynamic and kinetic studies reveal that, in reactions with O_2, $[(TMPA)Cu(RCN)]^+$ initially transforms to a spectroscopically detectable Cu/O_2 = 1:1 superoxo−copper(II) adduct $[(TMPA)Cu(O_2)]^+$, which further reacts rapidly with additional $[(TMPA)Cu(RCN)]^+$ to give $[\{(TMPA)Cu\}_2(O_2)]^{2+}$.[5−7] As a dinucleating analogue of TMPA, a sterically and electronically comparable dinucleating ligand, D^1 (Chart 1), was synthesized, in which two tripodal TMPA units were joined by a hydrocarbon linker group (−CH_2CH_2−).[6] Reaction of $[(D^1)Cu^{I}_2(RCN)_2]^{2+}$

Chart 1

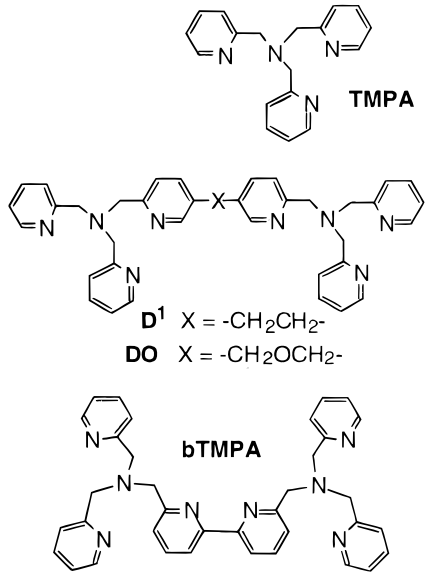

[⊗] Abstract published in *Advance ACS Abstracts*, October 15, 1997.

(1) Reviews emphasizing coordination models of dicopper protein sites: (a) Kitajima, N.; Moro-oka, Y. *Chem. Rev.* **1994**, *94*, 737−757. (b) Karlin, K. D. *Science* **1993**, *261*, 701−708. (c) Karlin, K. D.; Tyeklár, Z. *Adv. Inorg. Biochem.* **1994**, *9*, 123−172. (d) Karlin, K. D.; Tyeklár, Z.; Zuberbühler, A. D. Formation, Structure and Reactivity of Copper Dioxygen Complexes. In *Bioinorganic Catalysis*; Reedijk, J., Ed.; Marcel Dekker: New York, 1993; Chapter 9, pp 261−315. (e) Sorrell, T. N. *Tetrahedron* **1989**, *45*, 3−68. (e) Karlin, K. D.; Gultneh, Y. *Prog. Inorg. Chem.* **1987**, *35*, 219.

(2) Reviews emphasizing biochemical aspects of the dicopper protein sites: (a) Solomon, E. I.; Sundaram, U. M.; Machonkin, T. E. *Chem. Rev.* **1996**, *96*, 2563−2605 and references cited therein. (b) Fox, S.; Karlin, K. D. In *Active Oxygen: Reactive Oxygen Species in Biochemistry*; Valentine, J. S., Foote, C. S., Greenberg, A., Liebman, J. F., Eds.; Blackie Academic & Professional, Chapman & Hall: Glasgow, 1995; pp 188−231.

(3) (a) Tyeklár, Z.; Jacobson, R. R.; Wei, N.; Murthy, N. N.; Zubieta, J.; Karlin, K. D. *J. Am. Chem. Soc.* **1993**, *115*, 2677−2689. (b) Jacobson, R. R.; Tyeklár, Z.; Karlin, K. D.; Liu, S.; Zubieta, J. *J. Am. Chem. Soc.* **1988**, *110*, 3690−3692.

(4) Baldwin, M. J.; Ross, P. K.; Pate, J. E.; Tyeklár, Z.; Karlin, K. D.; Solomon, E. I. *J. Am. Chem. Soc.* **1991**, *113*, 8671−8679.

(5) (a) Karlin, K. D.; Wei, N.; Jung, B.; Kaderli, S.; Zuberbühler, A. D. *J. Am. Chem. Soc.* **1991**, *113*, 5868−5870. (b) Karlin, K. D.; Wei, N.; Jung, B.; Kaderli, S.; Niklaus, P.; Zuberbühler, A. D. *J. Am. Chem. Soc.* **1993**, *115*, 9506−9514.

S0020-1669(97)00639-3 CCC: $14.00

Chart 2

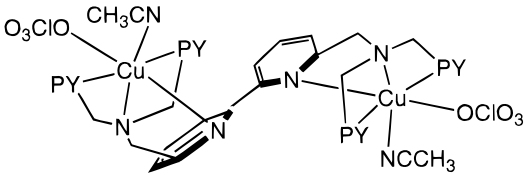

$[(bTMPA)Cu^{II}_2(CH_3CN)_2(ClO_4)_2]^{2+}$ (**1**)

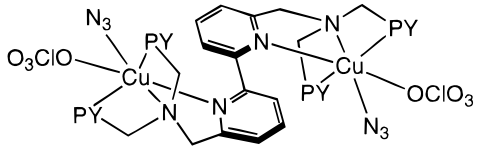

$[(bTMPA)Cu^{II}_2(N_3)_2(ClO_4)_2]$ (**2**)

$[(bTMPA)Cu^{I}_2]^{2+}$ (**3**)

with O_2 also gives a low-temperature metastable peroxo species $[(D^1)Cu_2(O_2)]^{2+}$, which is spectroscopically similar to $[\{(TMPA)Cu\}_2(O_2)]^{2+}$. A detailed kinetic and thermodynamic investigation revealed that the kinetic activation entropy and thermodynamic entropy of formation for $[(D^1)Cu_2(O_2)]^{2+}$ are considerably more favorable relative to those observed for $[\{(TMPA)Cu\}_2(O_2)]^{2+}$, and this is entirely because the dioxygen adduct is generated in an *intramolecular* fashion in the dinucleating system. However, this Cu_2-O_2 species is enthalpically destabilized compared to $[\{(TMPA)Cu\}_2(O_2)]^{2+}$; this is due to strain imposed by the $-CH_2CH_2-$ linker of dinucleating ligand D^1.[6−8] Most recent studies[6a] show that relief of strain is achieved by lengthening the linker,[8] and DO (Chart 1) can be employed to achieve room-temperature solution stability for $[(DO)Cu_2(O_2)]^{2+}$. The differences in mono- vs dinucleating copper complex chemistry observed attest to the great sensitivity of $Cu(I)/O_2$ binding and subsequent reactivity to detailed ligand environment modifications.

Thus, further variations in dinucleating ligand design are of interest. In this report, we describe the synthesis and characterization of new dicopper(I) and dicopper(II) complexes of a dinucleating analogue of TMPA, herein called bTMPA (Chart 1).[9] Here, two TMPA units are linked together directly, forming a 2,2′-bipyridine (bipy) moiety. Thus, the two chelating sites are potentially closer than in D^1. This ligand has been made before,[10] and Toftlund and co-workers have recently described a dicopper(II) and oxovanadium(IV) complex of bTMPA.[9] Here, the dinuclear copper(II) complexes $[(bTMPA)Cu^{II}_2(CH_3CN)_2(ClO_4)_2]^{2+}$ (**1**, as ClO_4^- salt) and $[(bTMPA)Cu^{II}_2(N_3)_2(ClO_4)_2]$ (**2**) were synthesized (Chart 2). Structures have been obtained by X-ray crystallography, and characterization in solution is made by UV−vis and EPR spectroscopy, while the electrochemical behavior of the complexes was determined by cyclic voltammetry in dimethylformamide. Since one of our primary interests is copper−dioxygen complexes and Cu^I_n/O_2 reactivity,[1b,c,7] we generated a dicopper(I) complex, $[(bTMPA)Cu^I_2](ClO_4)_2$ (**3**$(ClO_4)_2$) (Chart 2), and its reactivity toward dioxygen was tested.

Results and Discussion

Synthesis of bTMPA and Its Cu(II) and Cu(I) Complexes. The dinucleating ligand bTMPA was synthesized in a manner similar to that previously reported,[10] via reaction of 6,6′-(dibromomethyl)-2,2′-bipyridine[11a] with bis(picolyl)amine (PY1).[11b] The dinuclear Cu(II) complex $[(bTMPA)Cu_2(CH_3CN)_2(ClO_4)_2](ClO_4)_2\cdot 2CH_3CN$ (**1**$(ClO_4)_2\cdot 2CH_3CN$) was synthesized by reacting 2 equiv of $Cu(ClO_4)_2\cdot 6H_2O$ and the ligand bTMPA in acetonitrile (Experimental Section). Another dicopper(II) complex, $[(bTMPA)Cu_2(N_3)_2(ClO_4)_2]\cdot {}^1/_2CH_3OH$ (**2**$\cdot {}^1/_2CH_3OH$), was also generated following addition of sodium azide to the reaction carried out in methanol solvent.

A Cu(I) complex of the ligand was prepared in good yield by the addition of 2 equiv of $[Cu(CH_3CN)_4](ClO_4)$ to an acetonitrile solution of bTMPA under an argon atmosphere. According to ^1H NMR spectra and elemental analysis, the compound is formulated as $[(bTMPA)Cu^I_2](ClO_4)_2$ (**3**$(ClO_4)_2$), lacking coordinated nitrile ligands usually found with Cu(I)−TMPA containing ligand complexes.[5,6,12] The lack of an additional nitrile ligand in **3**$(ClO_4)_2$ may be due to the steric hindrance around the Cu(I) centers since the two chelate sites are very close to each other. Quinoline-containing analogues of TMPA, $[(BPQA)Cu](ClO_4)$ and $[(TMQA)Cu](ClO_4)$, in which two and three pyridines are replaced by quinolyl donors, respectively, were also found not to contain any coordinated nitrile ligand presumably due to the steric hindrance derived from the more bulky quinolyl donors.[13] Another possibility is that in bTMPA the tetradentate coordination is sufficiently altered from that in free TMPA, so that tetracoordination to Cu(I) is satisfied, precluding nitrile ligation; in $[(TMPA)Cu(CH_3CN)]^+$, the alkylamine donor binds only weakly.[3a] Complex $[(bTMPA)Cu^I_2](ClO_4)_2$ (**3**$(ClO_4)_2$) exhibits a ^1H NMR spectrum which has sharp, well-resolved signals (with small coordinated induced shifts) (Supporting Information). This contrasts to observations for the analogous mononuclear $[(TMPA)Cu(CH_3CN)]^+$ or dinuclear $[(D^1)Cu_2(CH_3CN)_2]^{2+}$ complexes, which show broadened spectra at room temperature; this has been ascribed to dynamic exchange behavior in the copper(I) complexes whose solid state structures exhibit pseudopentacoordination.[3a,6b] Due to the lack of crystallographic data for **3**$(ClO_4)_2$, it is impossible to determine the exact nature of the differences in coordination in this complex compared to those with TMPA or D^1 ligands. However, the absence of the coordinated acetonitrile and the sharp NMR spectrum suggest that the geometry about the copper atom in the complex is quite different.

X-ray Structure of $[(bTMPA)Cu_2(CH_3CN)_2(ClO_4)_2](ClO_4)_2\cdot 6CH_3CN\cdot 4H_2O$ (1-$(ClO_4)_2\cdot 6CH_3CN\cdot 4H_2O$). X-ray quality crystals, **1**$(ClO_4)_2\cdot 6CH_3CN\cdot 4H_2O$, were obtained by recrystallizing **1**$(ClO_4)_2\cdot 2CH_3CN$ from wet CH_3CN/Et_2O. A summary of crystal parameters and refinement results is given in Table 1, and selected bond lengths and angles are compiled in Table

(6) (a) Karlin, K. D.; Lee, D.-H.; Kaderli, S.; Zuberbühler, A. D. *Chem. Commun*. **1997**, 475−476. (b) Lee, D.-H.; Wei, N.; Murthy, N. N.; Tyeklár, Z.; Karlin, K. D.; Kaderli, S.; Jung, B.; Zuberbühler, A. D. *J. Am. Chem. Soc*. **1995**, *117*, 12489−12513. (c) Wei, N.; Lee, D.-H.; Murthy, N. N.; Tyeklár, Z.; Karlin, K. D.; Kaderli, S.; Jung, B.; Zuberbühler, A. D. *Inorg. Chem.* **1994**, *33*, 4625−4626.
(7) Karlin, K. D.; Kaderli, S.; Zuberbühler, A. D. *Acc. Chem. Res.* **1997**, *30*, 139−147.
(8) Comba, P.; Hilfenhaus, P.; Karlin, K. D., *Inorg. Chem.* **1997**, *36*, 2309−2313.
(9) Døssing, A.; Hazell, A.; Toftlund, H. *Acta Chem. Scand.* **1996**, *50*, 95−101. These researchers refer to the ligand as btpa.
(10) Dürr, H.; Zengerle, K.; Trierweiler, H. P. *Z. Naturforsch., B* **1988**, *43*, 361.
(11) (a) Rodriguez-Ubis, J.-C.; Alpha, B.; Plancherel, D.; Lehn, J.-M. *Helv. Chim. Acta* **1984**, *67*, 2265−2269. (b) Romary, J. K.; Zachairasen, D. R.; Barger, J. D.; Schiesser, H. *J. Chem. Soc. C* **1968**, 2884.
(12) Jacobson, R. R. Ph.D. Dissertation, State University of New York (SUNY) at Albany, 1989.
(13) Wei, N.; Murthy, N. N.; Chen, Q.; Zubieta, J.; Karlin, K. D. *Inorg. Chem.* **1994**, *33*, 1953−1965.

Table 1. Crystallographic Data for $[(bTMPA)Cu_2(CH_3CN)_2(ClO_4)_2](ClO_4)_2\cdot 6CH_3CN\cdot 4H_2O$ (**1**$(ClO_4)_2\cdot 6CH_3CN\cdot 4H_2O$) and $[(bTMPA)Cu_2(N_3)_2(ClO_4)_2]$ (**2**)

	1$(ClO_4)_2\cdot 6CH_3CN\cdot 4H_2O$	**2**
formula	$Cu_2C_{52}H_{66}N_{16}O_{20}Cl_4$	$Cu_2C_{36}H_{34}N_{14}O_8Cl_2$
temp, K	296	296
MW	1504.09	988.75
cryst syst	monoclinic	monoclinic
space group	*C*2/*c*	$P2_1/c$
a, Å[a]	15.907(4)	8.118(5)
b, Å	29.268(7)	29.743(8)
c, Å	13.941(2)	9.120(6)
β, deg	97.79(2)	114.00(5)
V, Å^3	6431(2)	2012(2)
F(000)	3104	1008
Z	4	2
λ(Mo Kα), Å	0.710 69	0.710 69
D_{calcd}, g/cm^3	1.553	1.632
abs coeff, cm^{-1}	9.11	12.61
scan type	$\omega-2\theta$	ω
rflns measd	$+h,+k,\pm l$	$+h,+k,\pm l$
rflns collected	4643	3895
indep rflns	4422	3635
no. of variables	325	280
R[a]	0.072	0.040
R_w[b]	0.086	0.046
goodness of fit[c]	4.46	1.57

[a] $R = \sum[|F_o| - |F_c|/\sum|F_o|]$. [b] $R_w = [\sum w(|F_o| - |F_c|)^2/\sum w|F_o|^2]^{1/2}$. [c] GOF $= [\sum w(|F_o| - |F_c|)^2/(NO - NV)]^{1/2}$.

Table 2. Selected Bond Distances (Å) and Angles (deg) for $[(bTMPA)Cu_2(CH_3CN)_2(ClO_4)_2](ClO_4)_2\cdot 6CH_3CN\cdot 4H_2O$ (**1**$(ClO_4)_2\cdot 6CH_3CN\cdot 4H_2O$) and $[(bTMPA)Cu_2(N_3)_2(ClO_4)_2]$ (**2**)

1$(ClO_4)_2\cdot 6CH_3CN\cdot 4H_2O$		**2**	
Intermolecular Distances (Å)			
Cu1−Cu1′	5.810(4)	Cu1−Cu1′	8.020(3)
Cu1−O1	2.63(1)	Cu1−O1	2.504(4)
Cu1−N1	2.05(1)	Cu1−N1	2.047(4)
Cu1−N2	2.02(1)	Cu1−N2	1.996(4)
Cu1−N3	1.99(1)	Cu1−N3	1.988(4)
Cu1−N4	2.42(1)	Cu1−N4	2.842(5)
Cu1−N5	1.98(1)	Cu1−N5	1.935(5)
N5−C51	1.15(2)	N5−C51	1.181(6)
Intermolecular Bond Angles (deg)			
N1−Cu1−N2	83.9(5)	N1−Cu1−N2	81.1(2)
N1−Cu1−N3	83.2(6)	N1−Cu1−N3	83.2(2)
N1−Cu1−N4	81.2(5)	N1−Cu1−N4	75.7(1)
N1−Cu1−N5	174.6(5)	N1−Cu1−N5	176.0(2)
N1−Cu1−O1	86.8(4)	N1−Cu1−O1	91.5(2)
N2−Cu1−N3	166.4(6)	N2−Cu1−N3	164.2(2)
N2−Cu1−N4	84.1(5)	N2−Cu1−N4	102.2(1)
N2−Cu1−N5	96.8(6)	N2−Cu1−N5	95.9(2)
N2−Cu1−O1	83.4(4)	N2−Cu1−O1	88.9(2)
N3−Cu1−N4	98.1(5)	N3−Cu1−N4	75.6(1)
N3−Cu1−N5	95.6(6)	N3−Cu1−N5	99.9(2)
N3−Cu1−O1	91.6(5)	N3−Cu1−O1	89.5(2)
N4−Cu1−N5	104.2(5)	N4−Cu1−N5	102.5(2)
N4−Cu1−O1	163.5(4)	N4−Cu1−O1	161.3(2)
N5−Cu1−O1	87.9(5)	N5−Cu1−O1	91.0(2)
Cu1−N5−C51	167(2)	Cu1−N5−N6	122.6(4)
N5−C51−C52	178(2)	N5−N6−N7	176.6(6)
Cu1−O1−Cl1	130.0(7)	Cu1−O1−Cl1	134.0(2)
O1−Cl1−O2	109.4(8)	O1−Cl1−O2	108.1(3)
O1−Cl1−O3	108.2(8)	O1−Cl1−O3	109.2(3)
O1−Cl1−O4	108.9(8)	O1−Cl1−O4	110.2(3)
O2−Cl1−O3	111(1)	O2−Cl1−O3	110.7(4)
O2−Cl1−O4	110.1(9)	O2−Cl1−O4	109.2(4)
O3−Cl1−O4	109(1)	O3−Cl1−O4	109.4(4)

2. A view of the cationic portion of the complex is depicted in Figure 1, including the atomic labeling scheme.

The dication molecule $[(bTMPA)Cu^{II}_2(CH_3CN)_2(ClO_4)_2]^{2+}$ (**1**) possesses two Cu(II) ion moieties, which are related by a crystallographic 2-fold axis with Cu1···Cu1′ = 5.81 Å. The

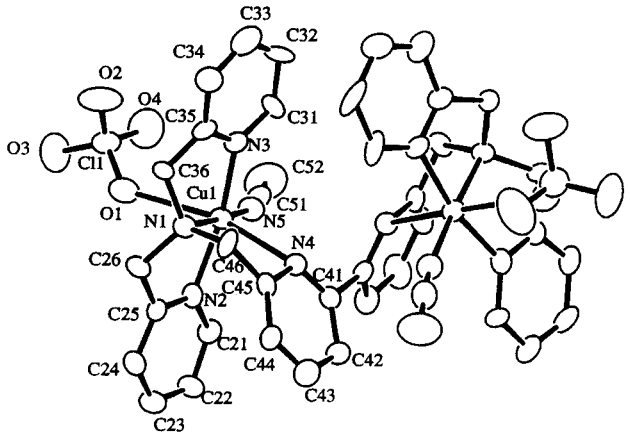

Figure 1. ORTEP diagram (20% ellipsoids) for $[(bTMPA)Cu_2(CH_3CN)_2(ClO_4)_2]^{2+}$ (**1**).

crystallographic 2-fold axis passes through the midpoint of the C41−C41′ (center of the bipy) vector; thus the coordination geometry around the two copper centers is identical. Each Cu(II) center is bonded to three pyridyl nitrogens, a nitrogen atom from the tertiary aliphatic amine, a nitrogen atom from an acetonitrile, and an oxygen atom from a bound perchlorate anion. The coordination geometry around each copper atom may be best described as pseudo-octahedral. The equatorial plane is composed of the aliphatic amine nitrogen (N1), two pyridyl donors (N2, N3), and the nitrogen from an acetonitrile. The plane formed has a maximum deviation from the least-squares plane of 0.015 Å. The copper atom lies 0.09 Å out of the basal plane toward the apical N_{py} (N4) atom. The other axial coordination site is occupied by the perchlorate oxygen atom O1. The interactions between the copper ion and the axial ligand atoms are weak, as expected for a Jahn−Teller distorted d^9 Cu(II) ion complex;[14] these distances are Cu1−O1 = 2.63(1) Å and Cu1−N4 =2.42(1) Å.

The average bond distance (2.02 Å) of the equatorial N_{py}−Cu is in the range expected for other related cupric compounds containing this same tripodal N_4 ligand.[12,15] The $Cu-N_{amine}$ bond length of 2.05 Å is close to one found in another structurally similar Cu(II) complex where a tertiary amine ligand is located in the basal plane of an octahedral.[16] The short $Cu-N_{acetonitrile}$ bond (1.98 Å), indicating strong binding of the nitrile group to the copper (II) center, closely matches that observed for the mononuclear complex $[(TMPA)Cu^{II}(CH_3CN)](ClO_4)_2$.[12]

An interesting structural feature is that the two covalently connected bipy pyridyl rings in the center of the structure are twisted at an angle of 47.5°, even though such an orientation is energetically less favorable due to the breaking of the π-conjugation. This twist apparently results because of nonbonded repulsions between the two chelating sites, especially the interaction between the equatorial pyridyl group containing N3 and the other one with N3′. Considerable steric repulsions occur: C33···C33′ (3.44 Å), C33···C32′ (3.54 Å), where those distances are close to the sum of the appropriate van der Waals radii. A simple hand-held molecular model shows that if basic structural factors (e.g., bond dstances and angles) were maintained but the two bipy pyridine rings were made coplanar, then the two equatorial pyridyl planes would be interlocking and each bound acetonitrile would also contact the pyridine plane

(14) Hathaway, B. J. In *Comprehensive Coordination Chemistry*; Wilkinson, G., Ed.; Pergamon: New York, 1987; Vol. 5, pp 533−774.
(15) Karlin, K. D.; Hayes, J. C.; Juen, S.; Hutchinson, J. P.; Zubieta, J. *Inorg. Chem.* **1982**, *21*, 4106−4108.
(16) Jacobson, R. R.; Tyeklar, Z.; Karlin, K. D.; Zubieta, J. *Inorg. Chem.* **1991**, *30*, 2035−2040.

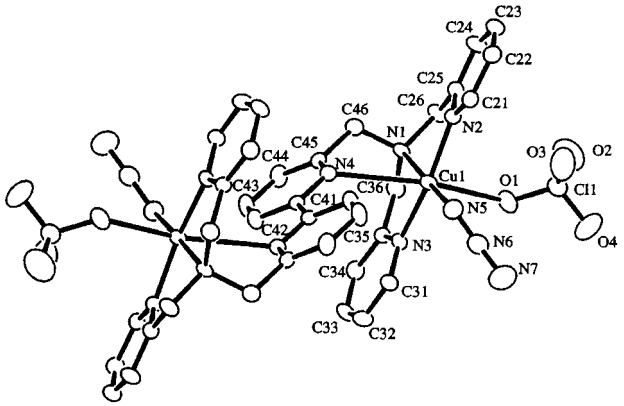

Figure 2. ORTEP diagram (20% ellipsoids) for $[(bTMPA)Cu_2(N_3)_2(ClO_4)_2]$ (**2**).

containing N4′. In an oxo−vanadium complex, $[(VO)_2(\mu\text{-}SO_4)(bTMPA)](ClO_4)_2 \cdot H_2O$, Toftlund and co-workers[9] also observe a twisting (79.7°) of the pyridines within the bipy moiety, and they further discuss the energetics involving this occurrence.

As mentioned, the axial N4−Cu bond distance (2.42 Å) is significantly longer than that of the equatorial Cu−N_{py} bonds. However, the axial Cu−N_{py} bond distance observed here (2.42 Å) is much greater than the distances of elongated pyridyl axial bonds seen in trigonal bipyramidal, square pyramidal, or octahedral Cu(II) complexes with similar tripodal amine/pyridyl ligands.[14,16] This additional elongation may also be explained by the steric repulsion of the two chelating sites. The longer the metal−N_{py} distance, the less unfavorable the interaction between the pyridyl group containing N3 and the other one with N3′. The fact that the axial pyridine ring plane is not parallel to the Cu1−N4 axis (e.g., ∠Cu1−N4−pyridyl plane = 120.9°) is also explained similarly. For strongly bound pyridine-containing metal complexes, the metal−N_{py} bond axis lies in the pyridine plane, to optimize overlap with the nitrogen lone pair.

The overall structure of the mononuclear half of **1** contrasts greatly with that of the mononuclear analogue, $[Cu^{II}(TMPA)(CH_3CN)](ClO_4)$, which has a trigonal bipyramidal structure with a noncoordinating counteranion.[12] As described here, we ascribe the difference to steric constraints caused by having two closely adjacent chelating sites in **1**.

X-ray Structure of $[(bTMPA)Cu_2(N_3)_2(ClO_4)_2]$ (2). A summary of crystal parameters and refinement results of **2** is presented in Table 1. Selected bond lengths and angles relevant to the copper coordination sphere are listed in Table 2. An ORTEP diagram of complex **2** is displayed in Figure 2. The structure consists of discrete neutral $[(bTMPA)Cu_2(N_3)_2(ClO_4)_2]$ units, in which the two copper(II) moieties have equivalent coordination environments, related by a crystallographic center of symmetry located midway between the two copper atoms and bisecting the C41−C41′ bond of the bipyridyl group; Cu···Cu = 8.020 Å.

Each copper atom in the molecule is six-coordinate, in a distorted pseudo-octahedral geometry. Apical positions of the octahedron are occupied by a weakly bound perchlorate anion and a bipy pyridyl nitrogen atom (N4) with ∠N4−Cu1−O1 = 161.3°. The equatorial plane is composed of two pyridyl nitrogens (N2, N3), the tertiary amine nitrogen (N1), and the azide nitrogen atom (N5). The cupric ion lies 0.005 Å out of this basal plane toward the perchlorate oxygen atom. The angles between the Cu atom and the four atoms of the equatorial plane deviate 6−9° from 90°. This small distortion from ideal square geometry may be due to internal strain in the tripodal ligand for which short methylene arms give five-membered chelate rings. The average Cu−N_{py} bond length (1.992 Å) is almost the same as that (1.992 Å) found in $\mathbf{1}(ClO_4)_2 \cdot 6CH_3CN \cdot 4H_2O$.

The equatorial azide ligand is nearly linear with ∠N5−N6−N7 = 176.6(6)° and with bond distances N5−N6 = 1.181(6) Å and N6−N7 = 1.148(7) Å. The two N−N bonds appear to be asymmetric, since the bond distances significantly differ beyond their estimated standard deviations. The outer N6−N7 bond distance falls within the range of the average ionic azide N−N distance of 1.154 ± 0.015 Å suggested by Evans, Yoffe, and Gray,[17] while the N5−N6 distance is a little longer than that. Where the azide is asymmetric, the long N−N distance always occurs between the middle nitrogen and the coordinated nitrogen,[18] as observed in the present case. The Cu−N−N angle of 122.6° for the terminal azide is as expected for an sp^2-hybridized nitrogen atom. The metal−azide bond distance (1.935 Å) agrees with Cu−N distances found in Cu(II) complexes containing a terminally bound azide ligand bound to a single metal.[18]

The bipyridyl planes of **2** are coplanar, while the two pyridyl nitrogens are on opposite sides, unlike the structure of **1** (Figure 1); the reason for this is not entirely clear. This may have to do with the presence of an azide ligand in **2**, instead of an acetonitrile as in **1**. Since the two ligands have different Cu−N−N(C) angles (∠Cu1−N5−C51 = 167° for **1** and ∠Cu−N−N = 122.6° for **2**), crystal packing may require the two compounds to have different geometries. The same coplanar structural feature for the bipy portion of bTMPA was observed by Toftlund and co-workers for a dicopper(II) complex with coordinated sulfate.[9]

Solution Conductivity. Molar conductivities of $[(bTMPA)Cu_2(CH_3CN)_2(ClO_4)_2](ClO_4)_2 \cdot 2CH_3CN$ ($\mathbf{1}(ClO_4)_2 \cdot 2CH_3CN$) and $[(bTMPA)Cu_2(N_3)_2(ClO_4)_2] \cdot {}^1/_2CH_3OH$ ($\mathbf{2} \cdot {}^1/_2CH_3OH$) were measured in acetonitrile solution at room temperature. On the basis of a molar conductance value of 463.8 Ω^{-1} cm^2 mol^{-1} for $\mathbf{1}(ClO_4)_2 \cdot 2CH_3CN$, this behaves as a 1:4 electrolyte,[19] indicating that in solution the dication dissociates to give a tetracation and noncoordinating perchlorate anions, while there are weak interactions between two perchlorate anions and copper(II) ions in the solid state as shown in the crystal structure. The result (247.4 Ω^{-1} cm^2 mol^{-1}) for $\mathbf{2} \cdot {}^1/_2CH_3OH$ shows that the compound exists in solution as a 1:2 electrolyte,[19] suggesting that one anion from each copper(II) ion dissociates in solution. From the observed solid state bonding distances, we suggest that the weakly coordinated perchlorate anions are more likely to dissociate than the strongly bound azide anions. This is also consistent with the solution UV−vis of **2**, which exhibits a strong charge-transfer band due the azide binding (vide infra).

Electronic Spectroscopy and Electron Paramagnetic Resonance Spectroscopy of the Copper(II) Complexes. UV−vis and EPR spectroscopies were also utilized to investigate the solution state properties of the Cu(II) complexes. UV−vis spectra for a series of pentacoordinate Cu(II) complexes containing tripodal tetradentate amine/pyridine ligands have been previously reported.[12,15,20] They possess weak and broad d−d absorption bands between 650 and 1000 nm, occasionally with intense high-energy charge-transfer absorptions near 300−350 nm. It is documented especially for complexes with ligands of the type described here that a single d−d band with a high-energy shoulder is indicative of a trigonal bipyramidal stereochemistry around copper(II) while an absorption envelope with

(17) Evans, B. L.; Yoffe, S. D.; Gray, P. *Chem. Rev.* **1957**, *59*, 515.
(18) Dori, Z.; Ziolo, R. F. *Chem. Rev.* **1973**, *73*, 247.
(19) Geary, W. J. *Coord. Chem. Rev.* **1971**, *7*, 81.
(20) Wei, N.; Murthy, N. N.; Karlin, K. D. *Inorg. Chem.* **1994**, *33*, 6093−6100.

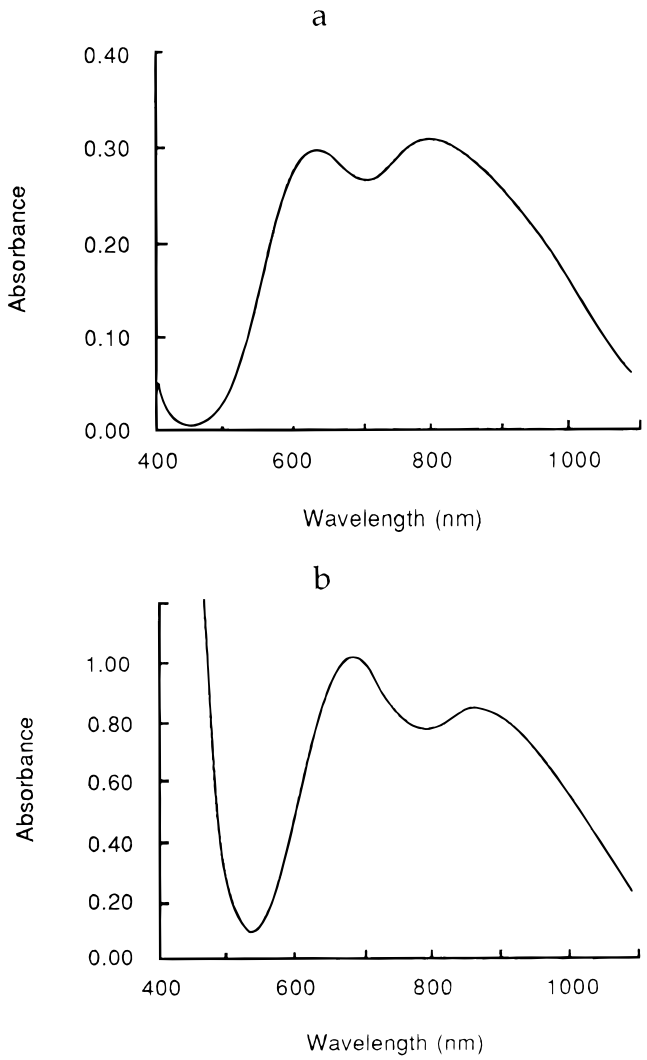

Figure 3. UV−visible spectra of cupric complexes in CH_3CN solvent: (a) $[(bTMPA)Cu_2(CH_3CN)_2(ClO_4)_2](ClO_4)_2 \cdot 2CH_3CN$ (**1**$(ClO_4)_2 \cdot 2CH_3CN$) and (b) $[(bTMPA)Cu_2(N_3)_2(ClO_4)_2] \cdot {}^1/_2CH_3OH$ (**2**$\cdot {}^1/_2CH_3OH$).

a low-energy shoulder is characteristic of a square pyramidal geometry.[12,14,15,21−25] Some pentacoordinate cupric complexes display two d−d band features of nearly equal intensity between 650 and 1000 nm, and these appear to possess an intermediate distorted geometry.[12,20]

The UV−visible spectra (Figure 3) of acetonitrile solutions of $[(bTMPA)Cu_2(CH_3CN)_2(ClO_4)_2](ClO_4)_2 \cdot 2CH_3CN$ (**1**$(ClO_4)_2 \cdot 2CH_3CN$) and $[(bTMPA)Cu_2(N_3)_2(ClO_4)_2] \cdot {}^1/_2CH_3OH$ (**2**$\cdot {}^1/_2CH_3OH$) exhibit two absorptions of nearly identical intensity in the range 630−870 nm. The azide-containing complex **2** also has a strong absorption at 422 nm ($\epsilon = 3180$) (Experimental Section), which can be confidently assigned as an azide-to-Cu(II) LMCT transition.[26] Consistent with the conductivity measurements (vide supra), the electronic spectra suggest that these Cu(II) complexes possess distorted solution structures, intermediate in geometry between pyramidal and trigonal bipyramidal. This contrasts with the solution (and also solid state) structures of the mononuclear analogue TMPA copper(II) complexes (e.g., $[(TMPA)Cu^{II}\text{-}X)]^{n+}$-X = Cl^-, CH_3CN), which are nearly perfectly trigonal bipyramidal.[12,15,20] Again, we suggest that this distortion can be explained by steric strain in the dinucleating ligand complex, which forces bulky chelating units to be in close proximity.

X-band EPR spectra of **1**$(ClO_4)_2 \cdot 2CH_3CN$ and **2**$\cdot {}^1/_2CH_3OH$ (Figure S2, Supporting Information) perfectly support the above picture of these complexes as having distorted pentacoordinate solution structures. The calculated spin-Hamiltonian parameters are summarized in Table 3. These frozen solution EPR spectra in DMF solvent are well-behaved and exhibit resolved spectra in the parallel region. They exhibit a spectral pattern characteristic of a $d_{x^2-y^2}$ ground state, i.e. tetragonal (axial), with $g_\parallel \sim 2.250 > g_\perp$ for **1** and $g_\parallel \sim 2.213 > g_\perp$ for **2**. This results are consistent with previous observations with pentacoordinate cupric complexes of tetradentate ligands, BPQA and BQPA (in which one or two pyridines are replaced by quinolyl donors), which, as suggested here, have distorted structures and display d−d UV−vis bands of nearly equal intensity and EPR signals typical of a tetragonal axial pattern.[20] By contrast, complexes with TMPA, e.g., $[(TMPA)Cu\text{-}X]^{2+/+}$ (X = Cl^-, CH_3CN, F^-, N_3^-) all possess a trigonal bipyramidal geometry, and the EPR spectra are quite different, displaying a "reversed" axial appearance.[12,15,20]

Electrochemistry. The electrochemical properties of compounds **1**−**3** and their mononuclear analogues have been studied by cyclic votammetry in dimethylformamide (DMF) with tetrabutylammonium perchlorate as the supporting electrolyte. Data, including the half-wave potential and peak separation for the compounds, are listed in Table 4, along with those of the related mononuclear TMPA complexes. Complexes **1**−**3** display a single quasi-reversible one-electron redox wave with $i_{pc}/i_{pa} \sim 0.8-1.0$. A typical cyclic voltammetric response exhibited by compound **1** is given Figure S3 (Supporting Information). A kinetic barrier to electron transfer at the electrode surface is indicated by extremely large peak separations (340−471 mV at a scan rate of 100 mV/s), which, however, decrease with decreasing scan rate. The ferrocene−ferrocenium couple showed $\Delta E_p = 62$ mV and $E_{1/2} = 545$ mV vs Ag/AgCl under the same conditions. From the cyclic voltammetry of the dicopper complexes **1**−**3**, only a single redox process of the two copper centers is observed, indicating that the two separate metal-associated redox processes occur at essentially the same potential. A study by Geiger and coworkers[27] showed that cyclic voltammetric scan rate changes may allow splitting of a two-electron CV wave into two distinctive peaks. However, when different scan rates were used for complexes **1**−**3**, no splitting of the redox was observed.

The half-wave potential for $[(bTMPA)Cu_2(CH_3CN)_2(ClO_4)_2](ClO_4) \cdot 2CH_3CN$ (**1**$(ClO_4)_2 \cdot 2CH_3CN$) is 180 mV, which is much higher (i.e., more positive) than that of the mononuclear analogue $[Cu(TMPA)CH_3CN)](ClO_4)_2$[12] ($E_{1/2} = -85$ mV) (Table 4). $[(bTMPA)Cu_2(N_3)_2(ClO_4)_2] \cdot {}^1/_2CH_3OH$ (**2**$\cdot {}^1/_2CH_3OH$) also has a much higher electrode redox potential ($E_{1/2} = -25$ mV) than a mononuclear analogue $[Cu(TMPA)(N_3)](ClO_4)$[12] ($E_{1/2} = -294$ mV). Complex **2** exhibits a more negative $E_{1/2}$ value than **1**, undoubtedly caused by the presence of the anionic azide ligand, which favors ligation to Cu(II) compared to Cu(I). The $E_{1/2}$ value of the Cu(I) complex $[(bTMPA)Cu^I_2](ClO_4)_2$ (**3**) is 199 mV. By contrast, the mononuclear [(TMPA)-

(21) (a) Thompson, L. K.; Ramaswamy, B. S.; Dawe, R. D. *Can. J. Chem.* **1978**, *56*, 1311. (b) Thompson, L. K.; Ramaswamy, B. S.; Seymout, E. A. *Can. J. Chem.* **1977**, *55*, 878.
(22) Duggan, M.; Ray, N.; Hathaway, B.; Tomlinson, G.; Briant, P.; Plein, K. *J. Chem. Soc., Dalton Trans.* **1980**, 1342.
(23) Addison, A. W.; Hendricks, H. M.; Reedijk, J.; Thompson, L. K. *Inorg. Chem.* **1981**, *20*, 102−110.
(24) Barbucci, R.; Bencini, A.; Gatteschi, D. *Inorg. Chem.* **1977**, *16*, 2117.
(25) Zubieta, J.; Karlin, K. D.; Hayes, J. C. In *Copper Coordination Chemistry: Biochemical and Inorganic Perspectives*; Karlin, K. D., Zubieta, J., Eds.; Adenine Press: Albany, NY, 1983; pp 97−108.
(26) Karlin, K. D.; Cohen, B. I.; Hayes, J. C.; Farooq, A.; Zubieta, J. *Inorg. Chem.* **1987**, *26*, 147−153.
(27) Pierce, D. T.; Geiger, W. E. *J. Am. Chem. Soc.* **1989**, *111*, 7636−7638.

Table 3. Electronic Spectral Data and EPR Parameters of Cu(II) Complexes

complexes	λ_{max}, nm (ϵ, $M^{-1}\,cm^{-1}$)[a]		EPR parameters[b]			
	d−d	CT	$g_{\|\|}$	$g_\perp$	$A_{\|\|}$[c]	$A_\perp$
$[(TMPA)Cu(CH_3CN)]^{2+}$ [d]	855 (254)		$g_{iso} = 2.099$			
$[(TMPA)Cu(N_3)]^{+}$ [d]	674 (277) 882 (275)	413 (2130)	2.002	2.181	76	92
$[(bTMPA)Cu_2(CH_3CN)_2(ClO_4)_2]^{2+}$ (**1**)	632 (171) 817 (164)		2.046	2.250	168	
$[(bTMPA)Cu_2(N_3)_2(ClO_4)_2]$ (**2**)	683 (352) 865 (290)	422 (3183)	2.044	2.213	176	

[a] CH_3CN solution. [b] Frozen glass (DMF) at 77 K. [c] $\times 10^4$ cm^{-1}. [d] Values from ref 12.

Table 4. Cyclic Voltammetric[a,b] Data for Copper Complexes **1**−**3**

compd	scan rate, V/s	$E_{1/2}$, mV	ΔE_p, mV	i_{pc}/i_{pa}
$[Cu^{II}_2(bTMPA)(CH_3CN)_2(ClO_4)_2]^{2+}$ (**1**)	0.1	181	433	1.01
$[Cu^{II}(TMPA)(CH_3CN)]^{2+}$	0.1	−85	87	0.85
$[Cu^{II}_2(bTMPA)(N_3)_2(ClO_4)_2]^{2+}$ (**2**)	0.1	−25	340	0.98
$[Cu^{II}(TMPA)(N_3)]^{+}$	0.1	−294	85	1.04
$[Cu^{I}_2(bTMPA)]^{2+}$ (**3**)	0.1	199	470	0.93
$[Cu^{I}(TMPA)(CH_3CN)]^{+}$	0.1	−78	91	1.05
ferrocene	0.1	545	62	1.00

[a] Glassy-carbon working electrode. [b] E (V) vs Ag/AgCl.

$Cu(RCN)]^+$ and another dinuclear analogue, $[(D^1)Cu_2(RCN)_2]^{2+}$,[6b] give values of −85 mV and −70 mV, respectively. Thus, our data reveals that the half-wave potentials of the bTMPA complexes, regardless of the copper oxidation state or the presence of additional ligands, are approximately 270 mV more positive than their mononuclear analogues.

Redox potentials of copper complexes are influenced by many factors, including the type of donor atoms and the geometry of coordinated complexes.[1e,19,26−31] Here, bTMPA complexes have the same donor atoms and chelate ring size as TMPA complexes. One effect that probably contributes to the much higher redox potential of the bTMPA complexes relative to the mononuclear complexes may be the occurrence of structural changes caused by the unfavorable steric interactions between pyridyl moieties, discussed earlier. Another explanation is that the bTMPA ligand is electron withdrawing compared to TMPA; this is reasonable since one pyridine donor (per copper ion) has an electron-withdrawing 2-(2-pyridyl)copper cationic substituent, which would thus favor a lower charged species, i.e., copper(I).

The Reactivity of $[(bTMPA)Cu^{I}_2](ClO_4)_2$ (3). This copper(I) complex is very stable toward dioxygen in the solid state. In acetonitrile solution, even when O_2 is directly bubbled through it at room temperature, the solution changes to green only very slowly (i.e., hours). The X-ray data of the Cu(II) complexes show that the copper ions of **1** and **2** can bind an acetonitrile and an azide ion, respectively, in their axial positions, indicating that molecular oxygen, which is smaller than acetonitrile or azide, should be able to bind to the copper(I) ions in **3**. However, the observed lack of coordination of nitrile ligands to **3** suggests that the copper(I) centers are not like that in TMPA analogues (vide supra), thus somehow altering reactivity. The lack of reactivity of $[(bTMPA)Cu^{I}_2](ClO_4)_2$ (**3**) toward O_2 reactions may be otherwise explained by electronic effects. The very positive $E_{1/2}$ potential indicates that this complex is difficult to oxidize and favors the Cu(I) oxidation state. This contrasts markedly with the behavior of $[(TMPA)Cu(RCN)]^+$, which reacts rapidly and reversibly with dioxygen to give $[\{(TMPA)Cu\}_2(O_2)]^{2+}$ even at very low temperatures (e.g., −80 °C).[6,7] A quinolyl derivative of TMPA, $[(TMQA)Cu]^+$, in which all three pyridyl substituents were replaced with quinolyl groups, has a much more positive potential than that of TMPA and also displays no dioxygen reactivity, that is, the ability to rapidly react with O_2 to give Cu_n-O_2 adducts.[13]

Summary and Conclusion

In this report, the synthesis and spectroscopic and electrochemical properties of dinuclear copper complexes with a dinucleating ligand, bTMPA, have been discussed. This ligand is a dinucleating analogue of TMPA where the two such units are covalently connected through one pyridine ring of each unit. Thus, the bipyridine (bipy) containing dinucleating ligand does not bind to a single copper ion via this strong chelating bidentate ligand, as previously observed by Toftlund and co-workers.[9] The two pyridines can be twisted with respect to one another, or they can be coplanar but with N atoms on opposite sides. Two cupric complexes, $[(bTMPA)Cu_2(CH_3CN)_2(ClO_4)_2](ClO_4)_2 \cdot 2CH_3CN$ (**1**$(ClO_4)_2 \cdot 2CH_3CN$) and $[(bTMPA)Cu_2(N_3)_2(ClO_4)_2] \cdot {}^1/_2CH_3OH$ (**2**$\cdot {}^1/_2CH_3OH$), have been synthesized. The solid state structures of these complexes were determined by X-ray crystallographic analyses. Steric hindrance created by proximity of the chelate sites influences the geometry around the copper ions and consequently causes the compounds to exhibit spectroscopic and electrochemical properties distinct from those of their parent TMPA analogues. UV−vis and EPR spectroscopy show that the complexes have distorted pentacoordinate structures in solution, contrary to the trigonal bipyramidal coordination generally seen for TMPA-containing Cu(II) complexes. Electrochemical measurements showed a significant effect (i.e., positive shift) of the Cu(II)/Cu(I) redox couple due to the steric hindrance of the ligand and/or an electron-withdrawing 2-(2-pyridyl)copper substituent on one pyridine ligand. This preference for Cu(I) oxidation state is one possible explanation for the lack of reactivity of $[(bTMPA)Cu^{I}_2](ClO_4)_2$ (**3**) toward dioxygen. While bTMPA has a deactivating effect toward copper(I)/O_2 reactivity, further studies of other di- or trinucleating analogues of TMPA are of continuing interest.

Experimental Section

Materials and Methods. Reagents and solvents used were of commercially available reagent grade quality unless otherwise stated. Acetonitrile was stirred over CaH_2 and then freshly distilled from CaH_2 under argon. Anhydrous diethyl ether was stirred over KOH and then distilled from sodium/benzophenone under argon or freshly dried by passing it through a 50 cm long column of activated alumina. Methanol was kept over 4 Å molecular sieves for 1 week and then freshly distilled from $Mg(OMe)_2$ under argon. All column chromatography of organic compounds was carried out by "flash chromatography" using either silica gel (60−200 mesh) or alumina (80−200 mesh). A 40 × 5 cm column was typically used. Fractions from column chromatography

(28) Miyoshi, K.; Tanaka, H.; Kimura, E.; Tsuboyama, S.; Murata, S.; Shimizu, H.; Ishizu, K. *Inorg. Chim. Acta* **1983**, *78*, 23−30.
(29) Karlin, K. D.; Sherman, S. E. *Inorg. Chim. Acta* **1982**, *65*, L39−L40.
(30) Augustin, M. A.; Yandell, J. K.; Addison, A. W.; Karlin, K. D. *Inorg. Chim. Acta* **1981**, *55*, L35.
(31) Patterson, G. S.; Holm, R. H. *Bioinorg. Chem*. **1975**, 257−275.

were monitored by using Baker-Flex IB-F (silica or aluminum oxide) TLC plates. Developed plates were analyzed by placing the plate in an iodine chamber or by a UV lamp (366 or 254 nm).

All air sensitive copper complexes were prepared and handled under an argon atmosphere using standard Schlenk techniques. Solvents and solutions were deoxygenated by either repeated vacuum/purge cycles using argon or bubbling of argon (20−30 min) directly through the solution. Samples for ^{1}H NMR and IR spectra were prepared in a Vacuum/Atmospheres drybox filled with argon.

Elemental analyses were performed by Desert Analytics, Tucson, AZ, and/or National Chemical Consulting Inc., Tenafly, NJ. Electroionization and chemical ionization mass spectra were obtained on a double-focusing Vacuum Generator 70-s (VG-70S) gas chromatography/mass spectrometer. Infrared spectra were recorded neat or in Nujol mulls on a Mattson Galaxy 4030 FT-IR spectrometer. ^{1}H NMR spectra were obtained in $CDCl_3$, CD_3CN, or CD_3NO_2 on a Bruker (300 MHz) spectrometer. All spectra were recorded in 5 mm o.d. NMR tubes. Chemical shifts were reported as δ values downfield from an internal standard of Me_4Si. Electrical conductivity measurements were carried out in acetonitrile solvent with a Barnstead Model PM-70CB conductivity bridge and a YSI Model 3403 conductivity cell. X-band EPR measurements were taken using a Varian E-4 spectrometer equipped with a liquid nitrogen Dewer insert. The field was calibrated with a powder sample of diphenylpicrylhydrazyl (DPPH; $g = 2.0037$). Frozen DMF solutions of copper complexes at $\sim 10^{-3}$ M in 4 mm o.d. quartz tubes were recorded. Electronic absorption spectra were taken with a Shimadzu UV-160 UV−vis spectrometer using quartz cuvettes (1 cm).

bTMPA Synthesis. This was synthesized according to the preparation previously descrcibed with some modification. To a solution of 6,6′-(dibromomethyl)-2,2′-bipyridine[11a] (0.57 g, 1.67 mmol) in 40 mL of tetrahydrofuran (THF) was added bis(picolyl)amine[11b] (0.66 g, 3.34 mmol). To the mixture was added Et_3N (0.85 g, 8.35 mmol). The reaction mixture was stirred at room temperature for 2 days. The white precipitate was filtered, and the solvent was removed on a rotary evaporator to give 1.14 g of a brown oil, which was purified by flash chromatography eluting with ethyl acetate on an alumina column ($R_f = 0.3$). Yield: 0.85 g, 88%. ^{1}H NMR ($CDCl_3$): δ 3.95 (s, 12H), 7.12 (m, 4H), 7.54 (d, 2H), 7.67 (m, 8H), 7.76 (t, 2H), 8.29 (d, 2H), 8.52 (m, 4H). Mass spectrum (CI/EI): m/z 579 $(M + 1)^+$.

CAUTION: *While we have experienced no problems in handling perchlorate salts, these should be handled with great caution due to the potential for explosion.*

[(bTMPA)$Cu_2(CH_3CN)_2(ClO_4)_2](ClO_4)_2\cdot 2CH_3CN$ ($1(ClO_4)_2\cdot 2CH_3CN$). A 100 mL Schlenk flask with a magnetic stirring bar was charged with copper perchlorate hexahydrate ($Cu(ClO_4)_2\cdot 6H_2O$) (0.13 g, 0.35 mmol). A 100 mL addition funnel was attached to the flask via a standard 14/20 joint, and the entire system was evacuated and purged three times with argon (to preclude moisture). A 7 mL acetonitrile solution of 0.11 g (0.129 mmol) of bTMPA was added to the funnel and then was bubbled with argon and added to the flask dropwise. This was stirred overnight at room temperature. Argon-saturated diethyl ether was added to the solution till it became cloudy (*ca*. 20 mL), and then the solution was filtered through a medium-porosity frit. Addition of another 75 mL of ether to the filtrate resulted in the separation of a blue solid. The clear solvent was decanted, and the solid was collected and then washed thoroughly with ether. The light blue powder obtained was recrystallized with CH_3CN to give 0.15 g of blue crystals (70%). Anal. Calcd for $Cu_2C_{44}H_{46}N_{12}Cl_4O_{16}$: C, 41.68; H, 3.66; N, 13.26. Found: C, 41.66; H, 3.62; N, 13.16. IR (Nujol; cm^{-1}): 2300 (CH_3CN), 2017 (ClO_4^- overtone), 1612 (C═C, aromatic), 1084 (ClO_4^-). UV−vis (CH_3CN; λ_{max}, nm (ϵ, M^{-1} cm^{-1})): 632 (171), 817 (164). Molar conductivity (CH_3CN): 463.8 Ω^{-1} cm^2 mol^{-1}. EPR (DMF): $g_{\|} = 2.250$, $A_{\|} = 168 \times 10^{-4}$ cm^{-1}, $g_{\perp} = 2.046$. X-ray quality crystals, $\mathbf{1}(ClO_4)_2\cdot 6CH_3CN\cdot 4H_2O$, were obtained by recrystallizing $\mathbf{1}(ClO_4)_2\cdot 2CH_3CN$ from wet CH_3CN/Et_2O.

Proof of the Presence of Solvated CH_3CN. KCN Reduction of Compound 1 in CD_3NO_2. Complex $\mathbf{1}(ClO_4)_2\cdot 2CH_3CN$ (0.13 g, 0.10 mmol) was dissolved in 2 mL of CD_3NO_2 in a small test tube containing 0.065 g (1.0 mmol) of KCN and a small stir bar. The tube was covered with a stopper and stirred at room temperature for 4 h. A yellowish brown colored solution formed, which was filtered into an NMR tube to record the spectrum. ^{1}H NMR (CD_3NO_2): δ 1.99 (s, 12H, $4CH_3$-CN), 3.97 (s, 12H), 7.0−7.32 (m, 4H), 7.54−7.80 (m, 12H), 8.53 (m, 4H).

[(bTMPA)$Cu_2(N_3)_2(ClO_4)_2]\cdot {}^1/_2CH_3OH$ ($2\cdot {}^1/_2CH_3OH$). (a) A methanolic suspension of NaN_3 (0.011 g, 0.17 mmol) was added to a solution of $\mathbf{1}\cdot 2CH_3CN$ (0.11 g, 0.087 mmol) in 25 mL of CH_3OH and stirred for 1 h. Distilled diethyl ether was added until the complex began to precipitate. The solution was filtered through a medium-porosity frit, and the complex was precipitated by the addition of 100 mL of diethyl ether. The supernatant was decanted, and the remaining solid was washed with 100 mL of additional diethyl ether. The product was recrystallized from methanol/ether to give 0.075 g (85%) of [(bTMPA)-$Cu_2(N_3)_2(ClO_4)_2]\cdot {}^1/_2CH_3OH$.

(b) The ligand bTMPA (0.20 g, 0.35 mmol) dissolved in 30 mL of methanol was added with stirring to solid $Cu(ClO_4)_2\cdot 6H_2O$ (0.26 g, 0.70 mmol). The resulting solution was stirred for 20 min, and then 20 mL of a methanolic solution of NaN_3 (0.046 g, 0.70 mmol) was added. The resulting green solution was stirred for 30 min. Diethyl ether (ca. 20 mL) was added to the solution until a slight cloudiness was observed, and then the mixture was filtered through a medium frit. An additional portion of diethyl ether (40 mL) was added to completely precipitate the green solid. The product was recrystallized from methanol/ether to give 0.29 g (82%) of product. Anal. Calcd for $Cu_2C_{36}H_{34}N_{14}Cl_2O_8\cdot {}^1/_2CH_3OH$: C, 43.34; H, 3.61; N, 19.51. Found: C, 43.11; H, 3.87; N, 19.28. IR (Nujol; cm^{-1}): 2052 (N_3^-), 1612 (C═C, aromatic), 1084 (ClO_4^-). UV−vis (CH_3CN; λ_{max}, nm (ϵ, M^{-1} cm^{-1})): 422 (3183), 683 (352), 865 (290). Molar conductivity (CH_3CN): 247.4 Ω^{-1} cm^2 mol^{-1}. EPR (DMF): $g_{\|} = 2.213$, $A_{\|} = 176 \times 10^{-4}$ cm^{-1}, $g_{\perp} = 2.044$.

Proof of the Presence of CH_3OH. KCN Reduction of Compound 2 in CD_3NO_2. The presence of CH_3OH in complex **2** was proved by NMR spectroscopy on a chemically reduced sample of the complex. Complex **2** (0.095 g, 0.095 mmol) was dissolved in 2 mL of CD_3NO_2 in a small test tube, and 0.061 g (0.95 mmol) of KCN was added. The tube was covered with a stopper and stirred at room temperature for 4 h. An orange yellowish colored solution was formed, which was filtered into an NMR tube, and a spectrum was recorded. ^{1}H NMR (CD_3-NO_2): δ 1.98 (br, CH_3OH), 3.3 (d, CH_3OH) 3.97 (s, 12H), 7.0−7.32 (m, 4H), 7.54−7.80 (m, 12H), 8.53 (m, 4H).

[(bTMPA)$Cu^I_2](ClO_4)_2$ (3). The ligand bTMPA (0.095 g, 0.16 mmol) was dissolved in 20 mL of argon-saturated CH_3CN and added dropwise to 0.11 g (0.32 mmol) of $[Cu^I(CH_3CN)_4](ClO_4)$ with stirring under argon for 25 min. To the resulting dark yellow solution was added air-free diethyl ether until the solution became cloudy (ca. 25 mL). The solution was then filtered through a medium-porosity frit and the complex precipitated by the addition of 40 mL of diethyl ether. The supernatant was decanted, and the complex was washed with 50 mL of additional diethyl ether. The resulting solid was recrystallized from acetonitrile/ether twice and dried under vacuum, giving 0.11 g (80% yield) bright yellow powder. Anal. Calcd for $Cu_2C_{29}H_{34}N_6$-Cl_2O_8: C, 47.79; H, 3.79; N, 12.39. Found: C, 47.40; H, 3.90; N, 11.93. ^{1}H NMR (CD_3CN): δ 4.06 (s, 8H), 4.38 (s, 4H), 7.17 (t, 4H), 7.27 (d, 4H), 7.68 (m, 6H), 7.86 (t, 2H), 8.00 (d, 2H), 8.34 (m, 4H). IR (Nujol; cm^{-1}): 1613 (C═C, aromatic), 1064 (ClO_4^-).

X-ray Structure Determination of [(bTMPA)$Cu_2(CH_3CN)_2(ClO_4)_2]$-$(ClO_4)_2\cdot 6CH_3CN\cdot 4H_2O$ ($1(ClO_4)_2\cdot 6CH_3CN\cdot 4H_2O$) and [(bTMPA)-$Cu_2$-$(N_3)_2(ClO_4)_2]$ (2). A blue cubic crystal of $\mathbf{1}(ClO_4)_2\cdot 6CH_3CN\cdot$-$4H_2O$, having approximate dimensions of 0.30 × 0.25 × 0.30 mm, was obtained from wet CH_3CN/ether (1:4) solution. A blue needle crystal of **2**, having approximate dimensions of 0.30 × 0.25 × 0.30 mm, was also collected from CH_3CN/ether (20:80) solution. These crystals were mounted on glass fibers. All measurements were made on a Rigaku AFC6S diffractometer with a graphite-monochromated Mo Kα source (λ(Mo Kα) = 0.710 69 Å). Cell constants and an orientation matrix for data collection were obtained from a least-squares refinement using the setting angles of 25 carefully centered reflections in the range $12.30° < 2\theta < 21.19°$ for $\mathbf{1}(ClO_4)_2\cdot 6CH_3CN\cdot 4H_2O$ and $20.19° < 2\theta < 28.92°$ for **2**. All data were collected at a temperature of 23 ± 1 °C using the $\omega-2\theta$ and the ω scan technique for $\mathbf{1}(ClO_4)_2\cdot 6CH_3CN\cdot 4H_2O$ and **2**, respectively, to a maximum 2θ value of 50.0°. In each case the intensities of three representative reflections which were measured after every 150 reflections remained constant

throughout data collection, indicating crystal and electronic stability. Thus, no decay correction was applied. All ORTEP diagrams were created by using the Johnson Programs (Johnson, C. K. ORTEPII. Report ORNL-5138; Oak Ridge National Laboratory, Oak Ridge, TN, 1976). Tables of crystal data, data collection methods, and refinement procedures are provided in Table 1.

Electrochemistry. Cyclic voltammetry was carried out by using a Bioanalytical Systems BAS-100B electrochemistry analyzer connected with a HP-7440A plotter. The cell consisted of a modification of a standard three-chambered design equipped for handling of air sensitive solutions by utilizing high-vacuum valves (Viton O-ring) seals. A glassy carbon electrode (GCE, BAS MF 2012) was used as the working electrode. The reference electrode was $Ag^+/AgCl$. The measurements were performed at room temperature under argon in DMF solvent containing 0.2 M tetrabutylammonium hexafluorophosphate (TBAHP) and $10^{-3}-10^{-4}$ M copper complex.

Acknowledgment. We thank the National Institutes of Health (GM 28962) for research support and the National Science Foundation (CHE-9000471) for help in the purchase of the X-ray diffractometer.

Supporting Information Available: Figure S1 depicting ^1H NMR spectra of bTMPA and $[(bTMPA)Cu_2]^{2+}(ClO_4)_2$ (**3**) at room temperature in acetonitrile, Figure S2 depicting EPR spectra of **1** and **2**, Figure S3 depicting the cyclic voltammogram of **1**, and full details of the X-ray structures of $\mathbf{1}(ClO_4)_2 \cdot 6CH_3CN \cdot 4H_2O$ and **2** with tables of atomic coordinates, bond lengths, and bond angles (16 pages). Ordering information is given on any current masthead page.

IC970639C